A Preliminary Demonstration of High Resolution Proximity Capacitance-Optical Multimodal CMOS Image Sensor

Tsubasa Nozaki[1], Yoshiaki Watanabe[1], Chia-Chi Kuo[1], Koga Saito[1], Takezo Mawaki[1, 2], Rihito Kuroda[1, 2]

tsubasa.nozaki.s7@dc.tohoku.ac.jp

[1] Graduate School of Engineering, Tohoku Univ., 6-6-05, Aza Aoba, Aramaki, Aoba-ku, Sendai, 980-8579, Japan

[2] New Industry Creation Hatchery Center, Tohoku Univ., 6-6-10 Aza Aoba, Aramaki, Aoba-ku, Sendai, 980-8579, Japan

Keywords: Proximity capacitance, Image sensor, Multimodal, Optical

ABSTRACT

This paper presents a preliminary demonstration of the proximity capacitance-optical multimodal imaging using a 2.8 μm-pitch 1.8M pixels CMOS image sensor. The experimental results showcase the high accuracy capacitance imaging, the good functionality of optical imaging, and the high spatial resolution, validating the feasibility of the multimodal imaging principle.

1 Introduction

Image sensors play an important role in acquiring information from the real world and the fields of applications are expanding in the era of big data. Among the many types of image sensors, proximity capacitance image sensors offer unique capabilities in visualizing two-dimensional distributions of capacitance between the sensor and targets. These sensors excel at detecting electrical connections and minute irregularities on objects, making them highly valuable in various fields. For instance, they are extensively used in wiring inspection for flat panel displays [1], fingerprint identification [2], biology analysis [3], and so on.

Meanwhile, multimodal image sensors are receiving great attentions for their ability to achieve high-functional imaging. These sensors combine multiple modalities to enhance the overall imaging capabilities. Practical applications include imaging of biological cells using ions and fluorescence [4], as well as imaging of the human body using PET and MRI [5].

For biological cell analysis, proximity capacitance imaging provides an ability to visualize biochemical reactions [3], while optical imaging enables identification and localization [6]. By integrating these two modalities through multimodal imaging techniques, it becomes possible to obtain comprehensive information about biological cells in a single imaging process. This approach enhances the precision and efficiency of image acquisition, leading to an improved understanding and analysis of cellular processes.

Previously, we presented a high-resolution proximity capacitance image sensor with 2.8 μm-pitch pixels [7]. This work expands the research by demonstrating the sensor's capability for proximity capacitance-optical multimodal imaging. The operation principle of the imaging technique and preliminary experimental results to verify the working principle are demonstrated as follows.

2 Operation Principle of Proximity Capacitance-Optical Multimodal Imaging

Figure 1 shows the circuit block diagram and pixel circuit of the prototype CMOS image sensor utilized for proximity capacitance-optical multimodal imaging in this work. The pixel consists of a detection electrode and a PN junction of transistor's source as a photodiode, allowing the acquisition of both capacitance and light signals. The sensor is operated by rolling shutter, where the pixel reset and row select are controlled by ΦR and ΦX, respectively. Each column S/H circuit is equipped with two capacitors, which are controlled by ΦN and ΦS.

Figure 2 shows a schematic diagram of the pixel cross-section and circuit schematic. Each pixel contains a parasitic capacitance; C_C at the detection electrode node. Note that during the capacitance imaging, the capacitance to be measured; C_S will be connected in series with C_C.

Figure 3(a) depicts the operating pulse diagram of capacitance imaging method. The ΦC represents the applied signal to the counter electrode of the target. After the pixel reset, two different voltage levels of ΦC are applied, and the corresponding output signals, V_{OUTN} and V_{OUTS}, are sampled in sequence. By using the differential output voltage, V_{OUT}, thermal noise and fixed pattern noise can be cancelled. The output signal is expressed by Eq. (1).

$$V_{OUT} = V_{OUTN} - V_{OUTS} = \frac{C_S}{C_S + C_C} \cdot V_{IN} \cdot G_{SF} \qquad (1)$$

where V_{IN} is the input pulse amplitude of ΦC, and G_{SF} is the gain of pixel source follower (SF).

Figure 3(b) shows the operation pulse diagram of optical imaging method. During the exposure, the PN junction of the source of the reset transistor, which is connected to the detection electrode node, functions as a photon-detector. After integrating the photo-generated electrons, the light signal voltage is read out as V_{OUTS}. Subsequently, the pixel reset is conducted and sampled as V_{OUTN}. This operation allows a sufficient exposure period for one frame. The output is expressed by Eq. (2).

$$V_{OUT} = V_{OUTN} - V_{OUTS} = \frac{Q}{C_S + C_C} \cdot G_{SF} \qquad (2)$$

where Q is the amount of the integrated photo-generated charges. When using the optical imaging method for proximity targets, C_S will vary for each pixel, depending on the distance between target and each detection electrode.

To demonstrate the proximity capacitance and optical imaging methods, we utilized a 2.8 μm-pitch 1.8M pixel CMOS image sensor fabricated using a 0.18 μm CMOS process, previously reported as a proximity capacitance CMOS image sensor [7]. Three types of characteristics were obtained; the input voltage to capacitance transfer characteristic, the photoelectric conversion characteristic in response to light, and the modulation transfer function (MTF) as an index of spatial resolution in both capacitance and optical imaging.

Figure 4 shows micrographs of the prototype chips employed for the experiments. Figure 4(a) shows the basic chip for measuring voltage-capacitance transfer characteristics and photo response. Figure 4(b) shows the chip with various metal wiring patterns formed on top of the sensor surface, for the measurement of MTF. The characteristics were obtained by lens-free proximity imaging.

Figure 5 shows the TEM image of the pixel cross-section of the fabricated chip, showing the wiring layers including the capacitance detection electrode. Note that for the prototype chip the optical aperture is almost zero for the normal incident light due to the metal wiring.

Figure 6 shows the photograph and block diagram of the measurement system.

3 Experimental Results and Discussion

The following are the measurement results of the proximity capacitance and optical imaging using the prototype chips.

3.1 Voltage-Capacitance Transfer Characteristics

Figure 7(a) shows the measurement setup and results of the voltage-capacitance transfer characteristics. During the experiment, the distance between the probe and the sensor was adjusted to tune different levels of capacitance C_S. The resulting output voltages obtained using capacitance imaging method, with the input pulse amplitude applied to the probe (V_{IN}), are plotted in Fig. 7(b). For the comparison, the solid black lines show the theoretical characteristics for typical capacitance values of C_S. The results demonstrate good linearity at a distance range of 0 to 5 mm from the sensor, indicating that the capacitance can be accurately detected for the range of aF to several zF.

3.2 Photoelectric Conversion Characteristic

Figure 8 shows the measured photoelectric conversion characteristic of the sensor across different illuminance levels. The observed response of the output voltage to the incident light confirms the functionality of the photon detector of the pixel circuit when employing the optical imaging method.

Note that in this experiment, a strong light source was applied to ensure a sufficient level of light signals. The relatively low light sensitivity can be attributed to the very low optical aperture of the chip, as illustrated in the TEM image in Fig. 5. The light sensitivity can be improved by modifying the metal wiring layout for higher aperture.

3.3 Modulation Transfer Function (MTF)

Figure 9 shows a 3D model of the sensor wiring and a simplified pixel output graph. The MTF is calculated using the minimum value (V_{min}) and the maximum value (V_{max}) of the output voltage at a specific spatial frequency ω, as described in Eq. (3).

$$MTF(\omega) = \frac{V_{max}(\omega) - V_{min}(\omega)}{V_{max}(\omega) + V_{min}(\omega)} \quad (3)$$

Figure 10 (a) and (b) shows the capacitance image and optical image, respectively, with the metal pattern formed on the chip surface during the back-end-of-line process for the MTF measurement. In the capacitance image, the brighter pixels represent larger capacitance values due to the metal pattern. On the contrary, in the optical image, the shaded pixels by metal pattern result in lower signal values and appear darker.

Figure 11 shows the experimental and theoretical MTF characteristic. For the capacitance and optical image acquisition, the MTF values were around 0.7 and 0.35, respectively at the Nyquist frequency of ~180 lp/mm, which was calculated from the pixel pitch of 2.8 μm and measured using a 5.6 μm pitch wiring pattern. However, when comparing the optical imaging characteristics to the theoretical values, it was observed that the characteristics start to deteriorate from around 50 lp/mm. This can be attributed to the low light sensitivity of the pixels and the optical crosstalk between pixels due to the undesired light reflection and scattering due to the metal layers above the photodiode. By increasing the optical aperture of the pixel layout, an improved light sensitivity and spatial resolution can be expected in the future.

4 Conclusions

This paper presented the principle of proximity capacitance-optical multimodal imaging using a same pixel structure, and demonstrated basic characteristics of multimodal imaging results using a prototype CMOS image sensor with 2.8 μm-pitch 1.8M pixels. The results verified the proposed principle works with good spatial resolution for lens-free proximity imaging. The low light sensitivity and spatial resolution compared to the proximity capacitance imaging attributed to the almost zero optical aperture of the fabricate chip. In the future, we plan to fabricate an image sensor with better optical performances. The multimodal images of capacitance and light obtained using the sensor will be useful in a wide range of fields, including analysis in biology.

Acknowledgements

The authors would like to greatly thank Y. Sugama for his effort on the chip design and LAPIS Semiconductor for chip fabrication.

References

[1] M. Koerdel, F. Alatas, A. Schick, K. Kragler, R. L. Weisfield, Stefan J. Rupitsch and Reinhard Lerch, "Contactless Inspection of Flat-Panel Displays and Detector Panels by Capacitive Coupling," IEEE Trans. Electron Devices, Vol. 58, No. 10, pp. 3453-3462 (2011).

[2] S.M. Jung, J. M. Nam, D. H. Yang and M. K. Lee, "A CMOS integrated capacitive fingerprint sensor with 32-bit RISC microcontroller," IEEE J.

Solid-State Circ., Vol. 40, No. 8, pp.1745-1750 (2005).
[3] N. Couniot, L. A. Francis and D. Flandre, "A 16 × 16 CMOS Capacitive Biosensor Array Towards Detection of Single Bacterial Cell," in IEEE Trans. Biomed. Circ. Syst., Vol. 10, No. 2, pp. 364-374 (2016).
[4] H. Nakazawa, M. Ishida and K. Sawada, "Multimodal bio-image sensor for real-time proton and fluorescence imaging," Sens. Actuators B: Chemical, Vol. 180, pp. 14-20 (2013).
[5] S. Vandenberghe and P. K. Marsden, "PET-MRI: a review of challenges and solutions in the development of integrated multimodality imaging," Phys. Med. Biol. Vol. 60, No. 4, p. R115 (2015).
[6] T. W. Su, S. Seo, A. Erlinger and A. Ozcan, "High-throughput lensfree imaging and characterization of a heterogeneous cell solution on a chip," Biotechnol. Bioeng., Vol. 102, pp. 856-868 (2009).
[7] Y. Sugama, Y. Watanabe, R. Kuroda, M. Yamamoto, T. Goto, T. Yasuda, H. Hamori, N. Kuriyama and S. Sugawa, "Two High-Precision Proximity Capacitance CMOS Image Sensors with Large Format and High Resolution," MDPI Sensors, Vol. 22, No. 7: 2770 (2022).

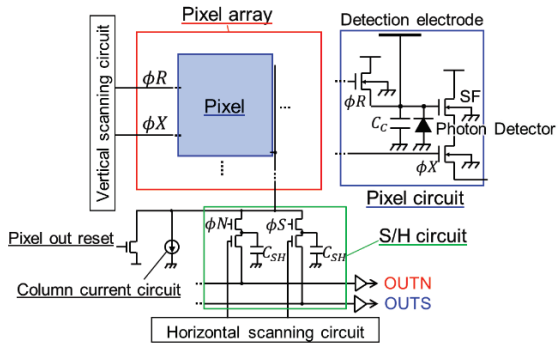

Fig. 1 Circuit block diagram and pixel circuit of the proximity capacitance image sensor.

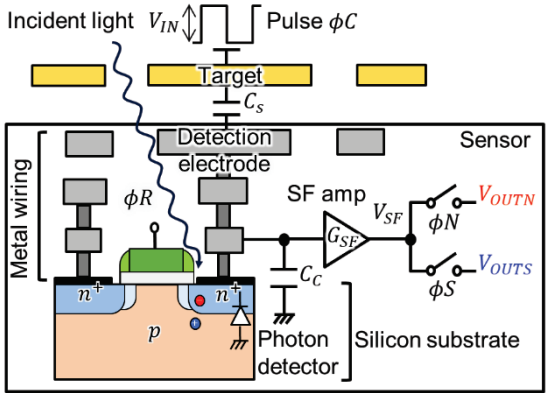

Fig. 2 Schematic diagram of pixel cross section and circuit.

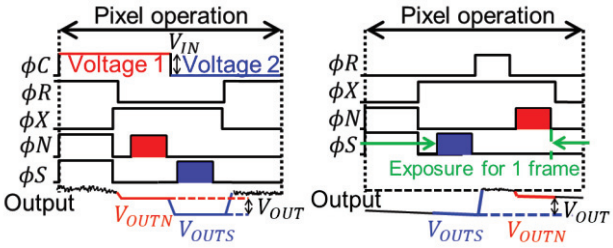

(a) (b)

Fig. 3 Operating pulse diagrams for (a) capacitance and (b) optical imaging.

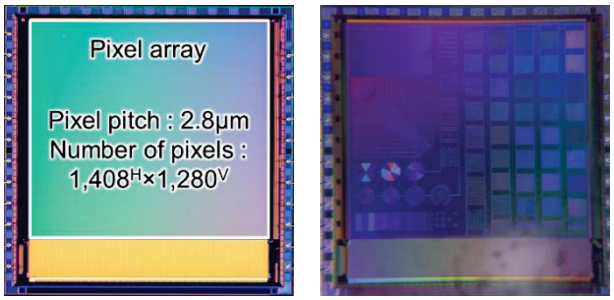

(a) (b)

Fig. 4 Micrograph of the chip used for the measurement.

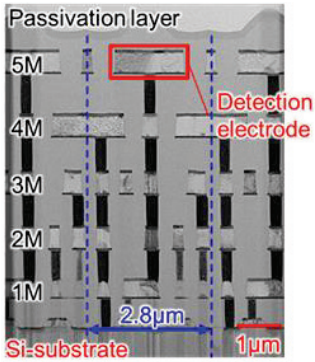

Fig. 5 Pixel cross-sectional TEM image of the chip in Fig. 4(a).

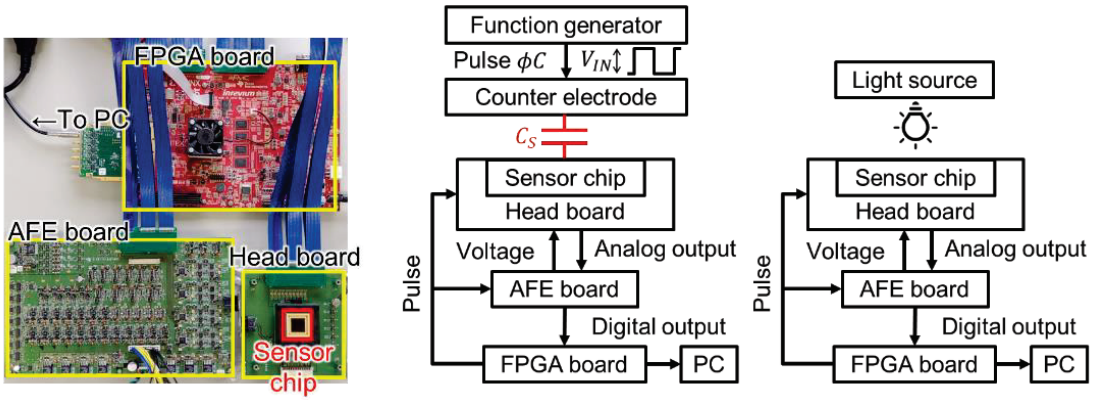

Fig. 6 Photograph and block diagram of the measurement system.

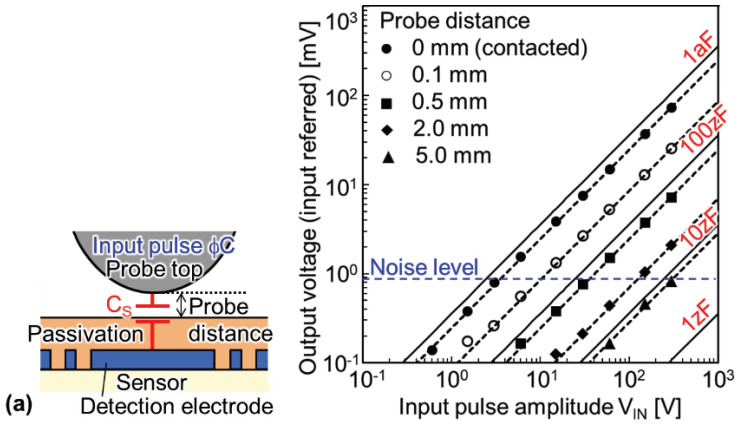

Fig. 7 Method and results of voltage-capacitance transfer characteristics with various capacitance range.

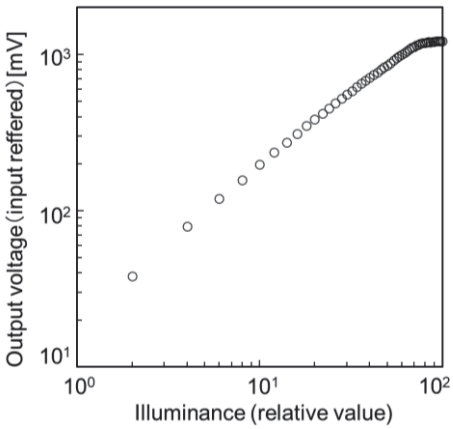

Fig. 8 Measurement results of photoelectric conversion characteristic.

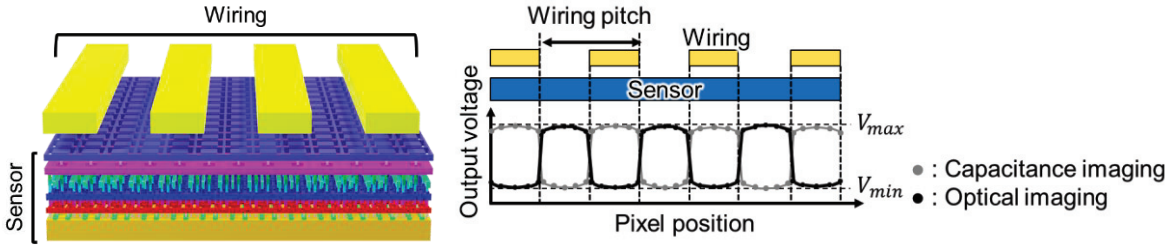

Fig. 9 3D model of a sensor with metal wirings on the surface and a simplified characteristics of capacitance and optical signal output under the metal wirings.

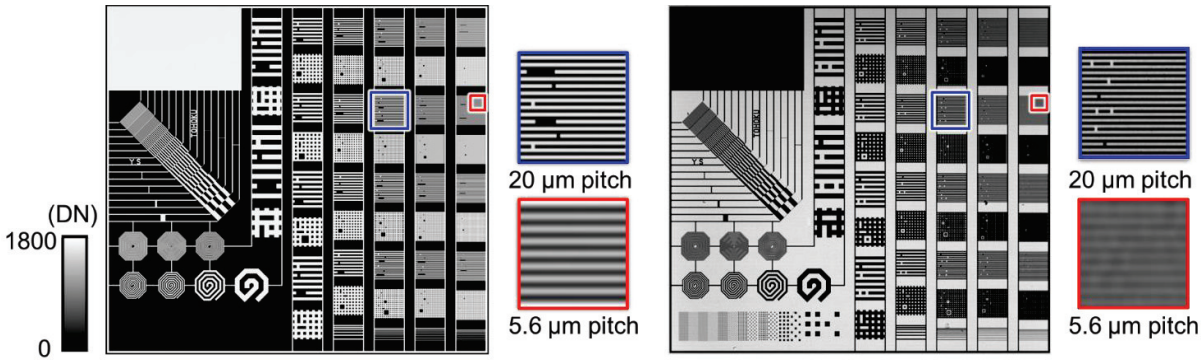

Fig. 10 (a) Capacitance and (b) optical images captured by the chips used for MTF measurements.

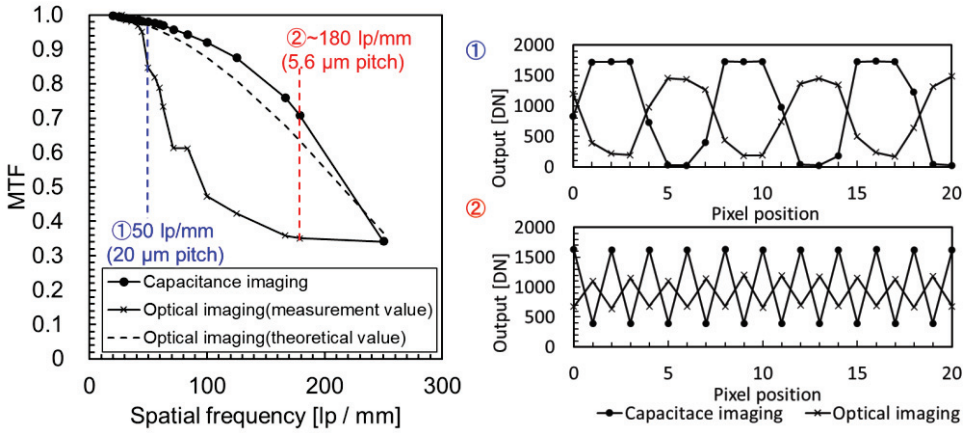

Fig. 11 Results of MTF measurements and pixel output values.